Multipath Fading in Wireless Sensor Networks: Measurements and Interpretation

Daniele Puccinelli and Martin Haenggi
Network Communication and Information Processing Laboratory
University of Notre Dame
Notre Dame, IN, USA
dpuccine@nd.edu, mhaenggi@nd.edu

ABSTRACT

Multipath fading heavily contributes to the unreliability of wireless links, causing fairly large deviations from link quality predictions based on path loss models; its impact on wireless sensor networks is considerable. Although analytical models provide a probabilistic description, multipath fading is a deterministic phenomenon. Moreover, in the case of static nodes, fading is time-invariant. We illustrate its spatial nature with experimental evidence obtained using lower-end sensing node hardware. We also show the limitations of the supposed immunity of wideband radios to multipath fading in indoor deployments.

Categories and Subject Descriptors: C.2.1 [Network Architecture and Design]: Wireless Communication

General Terms: Measurement, Experimentation.

Keywords: Multipath Fading, Rayleigh Fading, Wireless Propagation.

1. INTRODUCTION

Multipath fading has a distinct impact on the fragility of wireless links. It is considered a *small-scale* phenomenon in the sense that the level of attenuation of the signal changes substantially if the position of the receiver or the transmitter is varied by about half a wavelength. One of the most common features of wireless sensor networks is the fact that the nodes are usually static; *static multipath fading* is therefore of particular interest. Another physical phenomenon of interest is shadowing; it is considered a *large-scale* effect, as it corresponds to substantial deviations of the RF signal from its mean due to large obstacles, which create shadow zones that cause deep fades if a receiver happens to enter them.

Although the impact of multipath fading is particularly strong in rich scattering environments such as offices and other indoor locales, outdoor deployments of wireless sensing nodes are not immune to it. Radio waves still get reflected off buildings and other landscape features. Figure
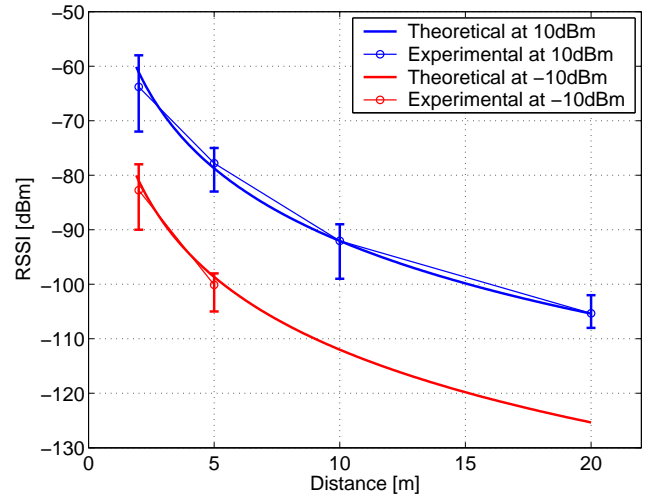
Figure 1: Signal strength for a point-to-point MICA2 link as a function of the internode distance in an outdoor environment. The signal strength is measured along circles of different radii centered at the transmitter; fading is responsible for the deviations from the mean value.

1 shows a number of received signal strength indications (RSSI) acquired with a transmitter/receiver pair of MICA2 motes in an outdoor environment; the nodes were placed on grass and signal strength was measured along circles of fixed radii centered at the transmitter. The mean values of the acquisitions along circles of different radii closely agree with the predictions of a path loss model [3] with a path loss exponent of 4.4, and the surprisingly large standard deviation of the measurements along circles of given radius is mostly due to multipath fading, even if radio anisotropy also plays a role [5].

In this paper, we illustrate some characteristic features of static multipath fading which are often overlooked. Common fading models are probabilistic, but fading itself is a deterministic phenomenon. In Section 2, after briefly summarizing the main probabilistic tools, we present a deterministic approach to multipath fading which does not lend itself to analytical developments, but offers the basis for a simulation study that leads to a better understanding of the phenomenon. Our focus is on lower-end sensing nodes, and our platforms are Crossbow's MICA2 and

MoteIV's Telos. MICA2 motes are built around an Atmel ATmega128L microprocessor and a narrowband radio (a 433MHz Chipcon CC1000 transceiver). The Telos platform uses an MSP430 microcontroller from Texas Instruments and is equipped with an IEEE 802.15.4-compliant 2.4GHz Chipcon CC2420 radio which uses spread spectrum techniques to increase channel reliability and noise tolerance by spreading the signal over a wider range of frequencies. In Section 3, the spatial nature of multipath fading is emphasized with the help of MICA2 and Telos hardware and a motorized turntable which we use to recreate multipath fading effects. This same tool is used in Section 4 to show how the probabilistic and the deterministic approaches to fading are indeed two sides of the same coin. Finally, Section 5 focuses on the behavior of wideband radios in the presence of multipath fading, and shows that such radios are not at all immune to it when deployed indoor.

2. DETERMINISM OF MULTIPATH FADING

The most commonly used fading models arise from dynamic contexts and consider fading from a probabilistic point of view. If we place a receiver at various positions in a rich scattering environment, the received signal measured by the receiver in each spot is the result of the superposition of all the scattered paths that reach it. In the absence of a dominating component, the envelope of the received signal can be shown to be Rayleigh-distributed [3]:

$$p_R(r) = \begin{cases} \frac{r}{\sigma^2} \exp\left(-\frac{r^2}{2\sigma^2}\right) & \text{if } r \geq 0 \\ 0 & \text{if } r < 0 \end{cases} \quad (1)$$

In the presence of a dominant, static component (typically a line-of-sight path), the envelope obeys a Ricean distribution. Its probability density may be written as

$$p_R(r) = \begin{cases} \frac{r}{\sigma^2} \exp\left(-\frac{(r^2+A^2)}{2\sigma^2}\right) I_0\left(\frac{Ar}{\sigma^2}\right) & \text{if } r \geq 0, \text{ with } A \geq 0 \\ 0 & \text{if } r < 0 \end{cases}$$
$$(2)$$

The parameter A provides an indication of the peak amplitude of the dominant path, and I_0 is the modified Bessel function of the first kind and zero-order. The Ricean factor K is defined as

$$K := 10 \log \frac{A^2}{2\sigma^2}.$$

As $A \to 0$ the Ricean distribution degenerates to a Rayleigh distribution (the dominant path vanishes).

Although a probabilistic approach is necessary for ease of tractability, fading is inherently deterministic. If we place a transmitter and a receiver in a room and allow them to communicate in the absence of external disturbances (such as motion of objects or people), the received signal strength is uniquely determined by the topology of the room and does not fluctuate in time. Time fluctuations come into the picture if the topology changes dynamically or if one of the terminals moves around: a mobile receiver will see a different topology depending on its position with respect to the transmitter. The motion of people or objects can be seen as a topology change and also causes time fluctuations.

Multipath fading depends on the topology of the environment where the nodes are deployed. The transmitted signal can reach the receiver by means of different paths depending on the position of the nodes and the layout of their surroundings.

Let us consider a wireless point-to-point setting, which can be generalized to a network. A transmitter T and a receiver R are deployed in a rich scattering environment. The position of the pair of nodes is determined by the two 3-tuples indicating their spatial coordinates with respect to a fixed reference, namely (x_T, y_T, z_T) and (x_R, y_R, z_R). If we assume a multipath channel with an additive white Gaussian noise process z, the signal from T received by R at time k is

$$y_k = a(x_T, y_T, z_T, x_R, y_R, z_R)x_k + z_k, \quad (3)$$

where a is the channel gain, determined by the large-scale path loss and the net effect of the multiple paths; a can be obtained experimentally by averaging y_k over time to eliminate the noise z_k.

Let us define a *fading function* [4] $f : \mathbb{R}^6 \to \mathbb{R}^+$ which deterministically maps the spatial coordinates of the transmitter and the receiver to a coefficient, modeling the effect of multipath fading. In a network with static nodes, the fading function associates a channel gain to the links between each node pair. Multipath fading favors some channels and penalizes others as a function of the position of the nodes; this is particularly relevant if the nodes are static (lack of time diversity). The fading function does not depend on time, and it does not incorporate the effects of the large scale path loss $L \propto d^{-\alpha}$, where α is the path loss exponent. Hence, the channel gain may be written as

$$a(x_T, y_T, z_T, x_R, y_R, z_R) = L \cdot f(x_T, y_T, z_T, x_R, y_R, z_R). \quad (4)$$

We will provide a clear illustration of these concepts by means of simulations as well as experimental results. We have created a simulator to compute the fading function for a two-dimensional setting where T occupies a fixed position within a rectangular room and R is placed at a number of different positions; in other words, our simulator computes a planar fading function $f_{2D} : \mathbb{R}^4 \to \mathbb{R}^+$ mapping (x_T, y_T, x_R, y_R) to a fading coefficient. The pair (x_T, y_T) is fixed, and (x_R, y_R) is allowed to vary in order to cover the two-dimensional topology. The output of the simulator is a mapping of the room where a signal strength level is associated with each point for a given position of the transmitter. The simulator traces N paths originating from T to check whether they reach R with reasonable strength (at least -110dBm, which is a typical sensitivity value for the kind of radios used in sensor node platforms). The power at a reference distance of 1m P_0 has been set to -50dBm on the basis of our experimental experience. Near-field effects are not taken into account. A wall attenuation factor of 10dB [3] has been chosen to account for the additional loss due to signal reflections off the walls. As for geometric ray tracing, it is assumed that the incidence and reflection angle are equal. Ray tracing is a well-established technique [3]; our simple simulator is not a contribution to such efforts, but a handy tool to illustrate the properties of the fading function.

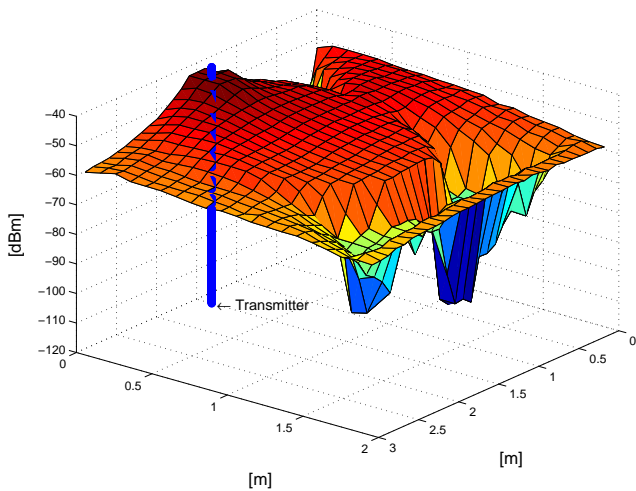As an example, we consider a rectangular topology model-

Figure 2: Simulated received power in a 3m × 2m rectangular geometry with a transmitter at (1.5m, 0.1m).

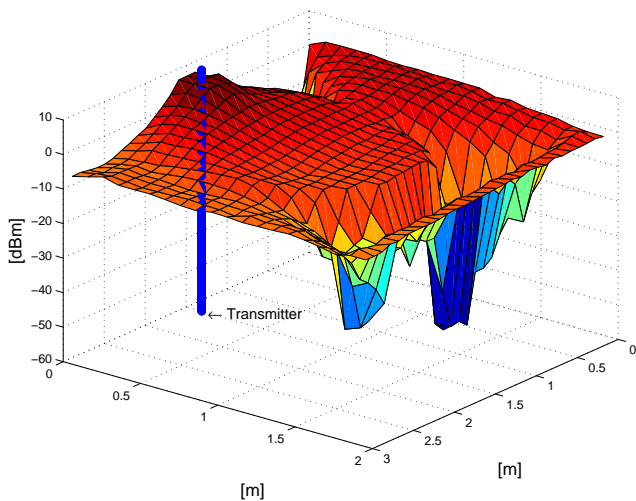**Figure 4: Simulated received power without the large-scale path loss with a transmitter at (2m, 1m).**

Figure 3: Simulated received power without the large-scale path loss with a transmitter at (1.5m, 0.1m).

ing a room measuring 3m × 2m. Figure 2 shows the received power when the transmitter is located in the position (1.5m, 0.1m) with respect to the indicated orthogonal coordinate system. The position of the transmitter is indicated by a bar. The product of the fading function and the large-scale path loss is simply a shifted version of the received power, as the transmitted power is constant. Figure 3 shows the received power without the large-scale path loss; comparing this figure with Figure 2 shows that multipath fading dominates over the large-scale path loss. This leads to the observation that the value of the path loss exponent is not that important so long as small distances (smaller than 10m) are considered.

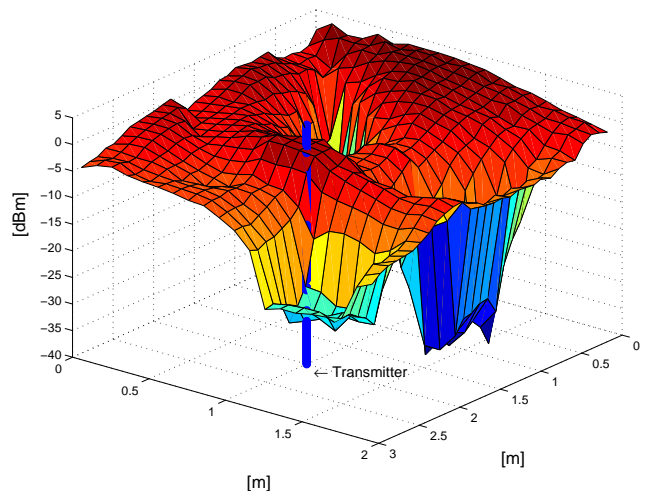With the help of the simulator we can also illustrate another important point: the fading function is a mapping from $\mathbb{R}^6$ ($\mathbb{R}^4$ with our two-dimensional simulator) to $\mathbb{R}$. The fading function assigns a different channel to different pairs of transmitters and receivers; therefore, the mapping pertaining to a given geometry changes depending on where the transmitter is located. In Figure 4 the geometry of the room is exactly the same as in Figures 2 and 3, but the transmitter has been moved to (2m, 1m), and this is enough to entirely modify the mapping. Surfaces such as the ones in Figures 3 and 4 only provide the mapping performed by the fading function for one position of the transmitter; as the transmitter moves, the surface keeps evolving: peaks form and merge back, troughs vanish and reappear.

3. SPATIAL NATURE OF MULTIPATH FADING

The two key points that we wish to illustrate in this section are the deterministic and spatial nature of multipath fading. We can use our simulator to measure the signal strength along a circle centered at some point in the room with the transmitter in a fixed position. We have also performed the same experiment with MICA2 hardware by placing the receiver on a motorized turntable. As the receiver occupies different positions along the circle, the fading function assigns a different channel gain to the transmitter-receiver pair. The channel is expected to change completely as the receiver moves by about $\lambda/2$, which is indeed the case in the simulation in Figure 5 where we have chosen $\lambda/2$=34.5cm (which corresponds to a carrier frequency of 433MHz, the same at which MICA2's CC1000 radio operates). As the receiver moves along the circle, it repeatedly occupies the same positions which are mapped to the same channels by the deterministic and time-independent fading function. We expect the waveform shown in Figure 5 to be repeated periodically, and we use sensor node hardware to verify this. Figure 6 shows the signal strength measured during a point-to-point transmission between MICA2 motes. For this particular experiment, a receiver was placed on a desk and a transmitter was located on the edge of a large motorized
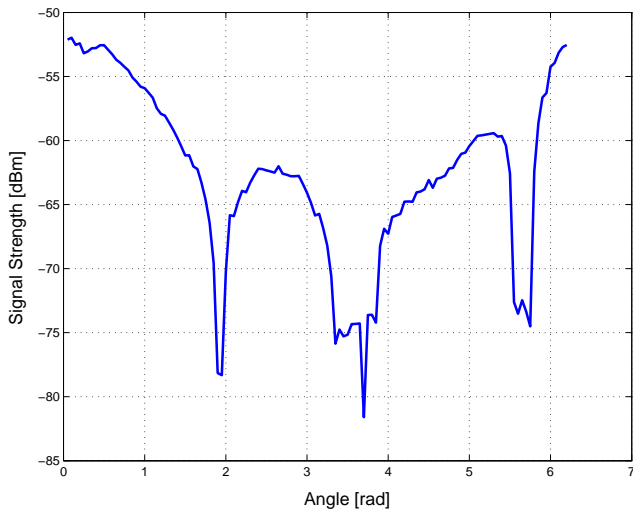
Figure 5: In this simulation, the receiver moves along a circle of radius 1m centered at (3m, 2m) in a rectangular environment of 3m × 2m with a transmitter at (2m, 2m). The carrier frequency is 433MHz, the same as in MICA2's CC1000 radio. As expected, a displacement of $\lambda/2$ (which here corresponds to 0.345rad) is sufficient to see a different channel.
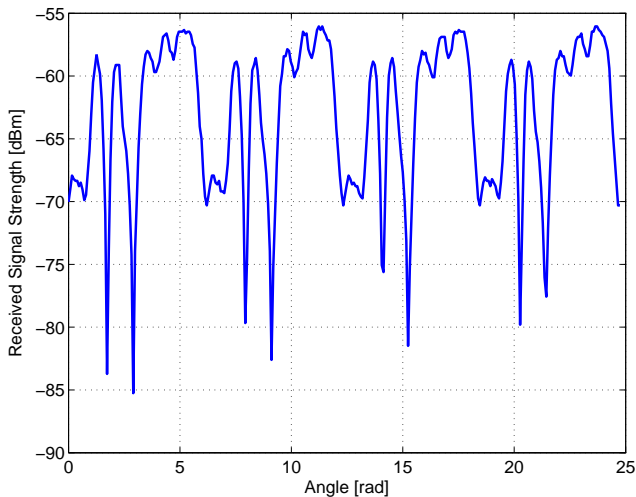

Figure 6: Measured signal strength with MICA2. The transmitter is located on a large motorized turntable, which rotates at 7.5rpm, and the receiver is placed on a desk.
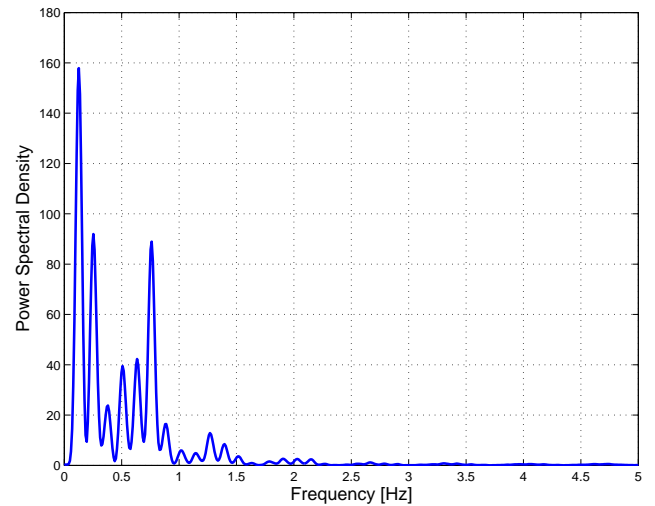

Figure 7: Power spectral density measured with MICA2 on a motorized turntable rotating at 7.5rpm.
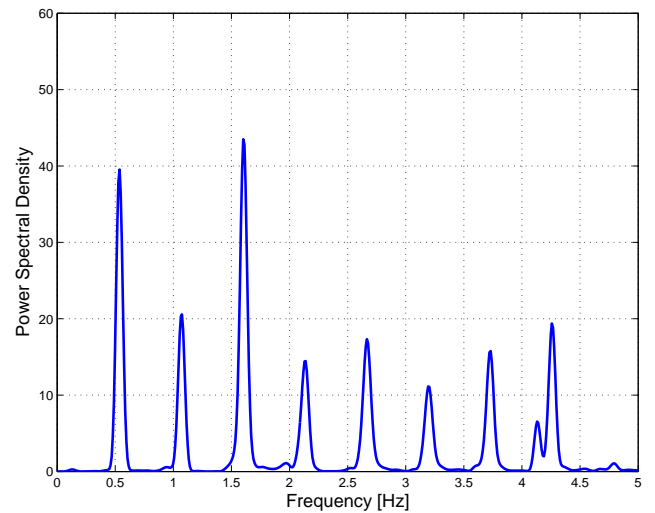
Figure 8: Power spectral density measured with MICA2 on a motorized turntable rotating at 32rpm.

turntable; a line-of-sight path was maintained between them at all times. The radius of the turntable is 0.61m, and it rotates at a speed of 7.5rpm; $\lambda/2$ corresponds to 0.57rad. From Figure 6, it is clear that the particular channel seen by the receiver only depends on the angle of the turntable. The signal shown is periodic for all practical purposes; it does not appear to be exactly periodic owing to quantization and sampling (the period of the revolution of the turntable is not an integer multiple of the sampling time). The level of

multipath fading for the link only depends on the position of the pair of nodes and the spatial characterization of the room. Since the time variations of the RSSI are uniquely due to the motion of the turntable, the rotational speed of the turntable directly influences the frequency contents of the RSSI; this can be clearly seen in the frequency domain in Figures 7 and 8. In the former, the turntable is revolving at 7.5rpm; it takes about 8 seconds to complete a revolution, and power density is therefore higher at integer multiples of $1/8 = 125$mHz. In the latter, the turntable moves at 32rpm, and it takes 1.86 seconds to complete a revolution; hence power density is higher at integer multiples of $1/1.86 = 538$mHz. This shows the spatial nature of fading from yet another point of view.
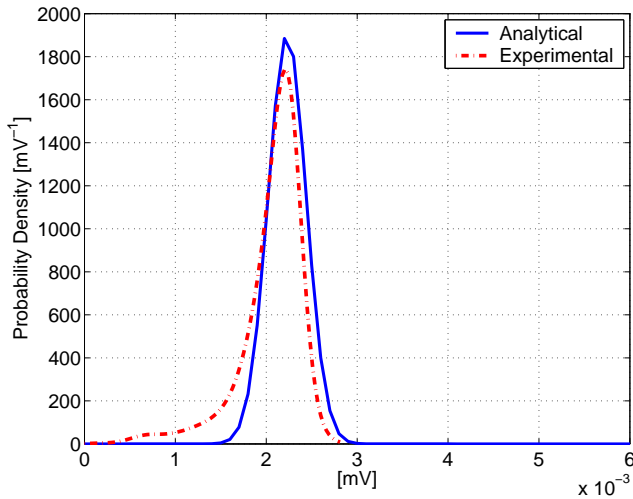
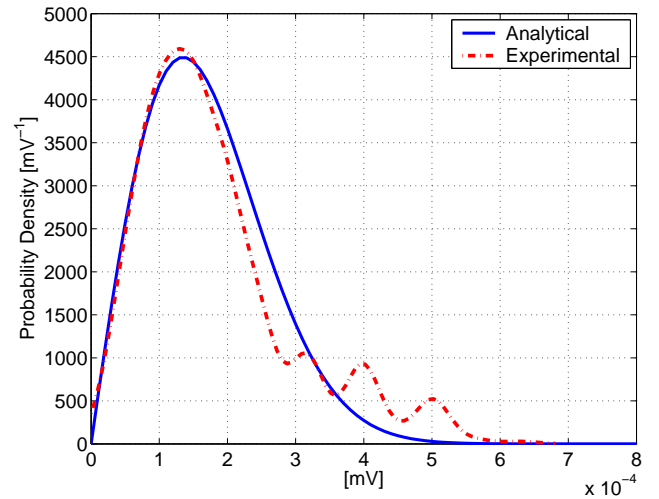Figure 9: Experimental verification of Ricean Fading with MICA2 hardware.

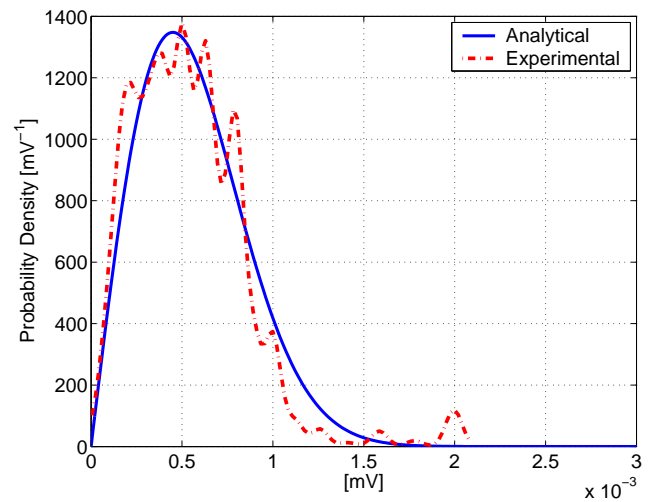Figure 10: Experimental verification of Rayleigh Fading with Telos hardware.

Figure 11: Rayleigh Fading with MICAz hardware: there remains a line-of-sight path, but it is comparable to a number of other multipath components.

4. THE CONVERGENCE OF THE PROBABILISTIC AND DETERMINISTIC APPROACHES

The probabilistic and deterministic viewpoint are two sides of the same coin. Since computing the fading function is too complex and topology-dependent, it makes sense to work out a probabilistic model. The probabilistic approach provides guidelines for the distribution of the received signal strength samples. The deterministic angle clarifies that the measured signal strength is not a random variable, but a deterministic quantity set by the topology of the environment.

Figure 9 refers to an experimental setting where both motes are on the turntable so that the dominant component is fully static, in harmony with the assumptions behind the Ricean model. The experimental data compare favorably with a Ricean probability density with $K = 17.5$dB. From an analytical standpoint, the Rayleigh model provides a wieldy tool for characterizing fading in a probabilistic fashion. The same cannot be said of the Ricean model, which provides a probability density featuring Bessel functions. The key to Rayleigh's simplicity is obviously the basic assumption of the absence of a dominant path.

Figure 10 shows the probability density measured during a turntable test with Telos motes along with a Rayleigh probability density with $\sigma = 1.35 \times 10^{-4}$mV. In this case, one mote was placed on the turntable, and the other was hidden inside a metal file cabinet. On average, they were 6m apart. Since there remains a trace of the direct path, the analytical curve does not quite match the experimental data in a section of the tail region.

The main assumption behind the Rayleigh model is that no path dominates at the receiver; this is reasonable in the absence of a line-of-sight path, but also in the presence thereof if the particular scattering properties of the surroundings of the network form a number of multipath components which are comparable in strength to the line-of-sight path. Figure 11 shows the match between an acquisition with MICAz hardware and a Rayleigh probability density with $\sigma = 4.5 \times 10^{-4}$mV obtained by placing the

turntable in a corner of a room. A line-of-sight is indeed present, but it does not stand out due to the specific geometry of the environment.

5. WIDEBAND RADIOS AND MULTIPATH FADING

Various techniques can be employed to counteract multipath fading, but they are not always effective. It is often assumed that a wideband radio is more immune to multipath fading than a narrowband radio [2]. If we look at the current status of sensor network research platforms, platforms such as Mica and MICA2 have narrowband radios, whereas Telos and MICAz have a wideband radio, Chipcon's CC2420.
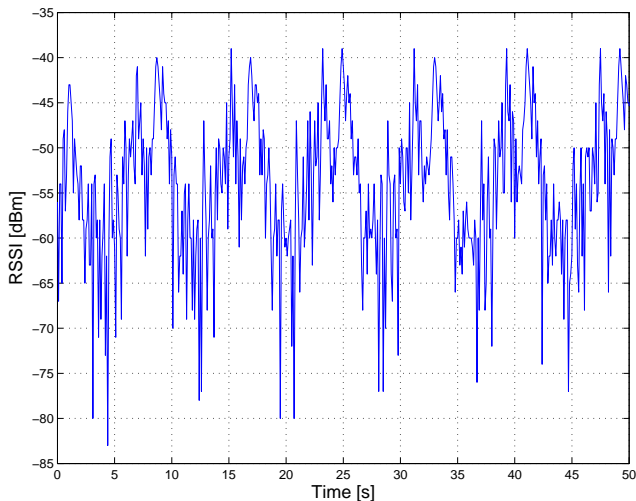
Figure 12: Measured signal strength with Telos.

The CC2420 has a carrier frequency of 2.4GHz and operates direct sequence spread spectrum with a spreading gain of 9dB; it is often pointed out how solidly it can mitigate multipath fading.

In a wireless channel, the delay spread Δt represents the time it takes the radio signal to cover the path difference Δl. The phase change relative to Δl is given by

$$\frac{\Delta l}{\lambda} = \Delta t \cdot c \cdot \frac{f}{c} = \Delta t \cdot f. \qquad (5)$$

If $\Delta l/\lambda = 1$, the phase changes by 2π, and we can define the coherence bandwidth [3] as

$$W_c \approx \frac{1}{2\pi\Delta t}, \qquad (6)$$

where

$$\Delta t = \frac{\Delta l}{\lambda \cdot f} \qquad (7)$$

The path difference Δl depends on the topology of the environment where the nodes are deployed. For indoor locales such as offices, 5m is a good estimate, and a reasonable value for the coherence bandwidth is thus W_c=10MHz. The CC1000 radio on the MICA2 motes has a radio signal bandwidth of less than 100kHz, which is considerably smaller than the coherence bandwidth of the channel and causes flat fading. In the case of the CC2420 on MICAz and Telos, the signal bandwidth is about 1MHz, which is still an order of magnitude below the channel coherence bandwidth: it is to be expected that the use of direct sequence spread spectrum will not help. This expectation is indeed confirmed by a simple turntable test performed with a pair of Telos motes. Figure 12 shows the received signal, affected by multipath fading in a measure perfectly comparable to the case of MICA2. The most evident difference is the smaller coherence time, due to the shorter wavelength. In this acquisition, the turntable rotates at 7.5rpm. Since the carrier frequency is 2.4GHz, $\lambda/2$ is approximately 6cm and corresponds to 0.1rad on this plot.

6. CONCLUSIONS

Multipath fading and shadowing contribute to the volatility of wireless links and must be accounted for when modeling the wireless channel. When the analysis of a higher-layer scheme (typically medium access and routing algorithms) is carried out, realistic assumptions must be made about the physical layer. The large-scale path loss is often used to identify an area of successful reception according to the so-called disc model [1], but this approach is strongly inadequate for the description of wireless sensor networks, as it overlooks the large deviation between the strength of signals measured by receivers equidistant from a transmitter. The Rayleigh fading model assumes the absence of a dominant path, whereas it is often the case that sensor nodes are linked by a line-of-sight path; however, its analytical tractability presents it as a very reasonable compromise between the simplistic disc model and the unwieldy Ricean fading model; moreover, the fact that it assumes the absence of a dominating line-of-sight path makes it a worst-case model.

Through a number of examples from simulations as well as experiments, we emphasize that fading is a spatial phenomenon. Under static conditions and in the absence of interference, wireless links provide a constant packet delivery performance. Time variations in signal strength only occur if the wireless terminals are moving or in the case of external disturbances; such fluctuations translate to a varying reception probability which directly impacts packet delivery performance. Fading does not directly depend on time, and only depends on the position of the nodes and the topology of their surroundings. For this reason, we introduce a *fading function* to describe the mapping between spatial coordinates and fading levels. Rayleigh and Ricean fading models operate a probabilistic description to abstract from the topology of networks and their surroundings; however, in principle, fading levels can be deterministically computed if the position of the terminals and the geometry of the environment where the network is deployed are known at all times. Although probabilistic models are very useful to describe wireless links, the true nature of fading should not be ignored.

We complement our collection of caveats against misconceptions on fading by also showing that the common belief that wideband radios help counteract fading does not really hold true in rich scattering environments.

7. REFERENCES

[1] E. N. Gilbert. Random plane networks. *Journal of SIAM*, 9:533–543, Oct. 1961.

[2] R. Kohno, R. Median, and L. B. Milstein. Spread Spectrum Access Methods for Wireless Communications. *IEEE Communications Magazine*, 33(1):58–67, 1995.

[3] T. S. Rappaport. *Wireless Communications.* Prentice Hall, Upper Saddle River, NJ, 2001.

[4] R.-H. Wu, Y.-H. Lee, and S.-A. Chen. Planning system for indoor wireless network. *IEEE Transactions on Consumer Electronics*, 47(1):73–79, 2001.

[5] G. Zhou, T. He, S. Krishnamurthy, and J. Stankovic. Impact of Radio Irregularity on Wireless Sensor Networks. In *The Second International Conference on Mobile Systems, Applications, and Services (MobiSys'04)*, Boston, MA, June 2004.